ISBN: 978-3-95450-247-9 ISSN: 2673-5490 doi: 10.18429/JACoW-IPAC2024-WEPG83

DEVELOPMENT OF AN ACTIVE BEAM-STABILIZATION SYSTEM FOR ELECTROFISSION EXPERIMENTS AT THE S-DALINAC*

D. Schneider†, M. Arnold, J. Birkhan, U. Bonnes, A. Brauch, M. Dutine, R. Grewe, L. E. Jürgensen, N. Pietralla, F. Schliessmann, G. Steinhilber
Technische Universität Darmstadt, Institute for Nuclear Physics, Darmstadt, Germany

Abstract

The r-process fission cycle terminates the synthesis of heavy elements in binary neutron-star mergers. Fission processes of transuranium nuclides are planned to be studied in electrofission reactions at the thrice-recirculating electron accelerator S-DALINAC. Due to the miniscule fissile target, the experimental setup requires an active beam-stabilization system with high accuracy and a beam position resolution in the submillimeter range. Requirements and concepts for this system regarding beam diagnostics elements, feedback control and readout electronics will be presented. The usage of a cavity beam position monitor and optical transition radiation screens to monitor the required beam parameters will be discussed in detail. Additionally, various measurements including a first study of beam stability performed in the injector section of the S-DALINAC to assess requirements and limits for the beam-stabilization system will be presented. Finally, the possible application of advanced machine-learning methods, such as neural networks and agent-based reinforcement learning, will be discussed.

INTRODUCTION

The superconducting Darmstadt electron linear accelerator (S-DALINAC) at the Institute for Nuclear Physics at the Technische Universität Darmstadt is used for scientific research in nuclear spectroscopy and meteorology, nuclear astrophysics and accelerator science [1] and can be operated in energy-recovery modes [2–4]. The current layout of the S-DALINAC is shown in Fig. 1. Due to its superconducting design the accelerator is able to provide a continuous-wave electron beam at a frequency of 3 GHz with a kinetic design energy of up to 130 MeV. The beam quality can be further improved by using the scraper systems located in both the low and high energy sections to reach the minimum design energy spread of 10^{-4} with bunch lengths of smaller than 2 ps [5, 6]. The electron beam can be utilized at various experimental setups including the QCLAM magnet spectrometer. Multiple high-resolution (e,e') and (e,e'γ) coincidence experiments have been conducted successfully at the QCLAM [7, 8].

A new series of measurements based on electron-induced fission at S-DALINAC is proposed to aim at a better understanding of the natural synthesis of heavy elements in our universe. While the details of the proposed experiment are provided in the following section, the requirements for the accelerator facility are challenging due to the miniscule radioactive target diameter of 1 mm, the request of ultra-short bunch lengths in the order of 1 ps and the demand for stable beam conditions for several hundred hours of measurement.

Therefore, a new active beam-stabilization system has been designed for electrofission experiments at the QCLAM magnet spectrometer. This project involves the commissioning of beam diagnostics elements and correction magnets including an in-house developed beam position and phase monitor. The focus is on utilizing existing in-house developed hardware and electronics. As feedback control algorithm both the performance of traditional proportional–integral–derivative (PID) controllers and machine-learning methods will be assessed.

ELECTROFISSION AT THE S-DALINAC

In order to investigate fission reactions of actinides and their dependence on the excitation energy of the nucleus and its angular momentum, electron-induced fission will be employed at the S-DALINAC. It allows the determination of the excitation energy of the actinide target nucleus. Additionally, higher multipoles can be excited and studied.

A schematic representation of the proposed electrofission setup is shown in Fig. 2. The electron beam will be provided with a beam current of 3 µA, electron energies in the order of 100 MeV and a 3σ beam spot size smaller than 1 mm at the electrofission interaction point. The electrofission target has a diameter of 1 mm and a target thickness of approx. 350 µg/cm^2. After its interaction with an electron the target nuclei can decay via fission. An accurate description of this process, which is not available up to date, requires the measurement of both fission fragments in coincidence. While e.g. photon-induced fission primarily excites E1 transitions, in electrofission higher multipole orders such as E2 and E3 can be exited [9]. As electron scattering experiments allow the decoupling of excitation energy and momentum transfer, a model-independent multipole decomposition using the electrofission cross section [10]

$$\frac{\mathrm{d}^2\sigma_\mathrm{f}}{\mathrm{d}\omega\,\mathrm{d}\Omega_\mathrm{e}} = \sigma_\mathrm{M} \sum_{\lambda=0}^{\infty} P_\mathrm{f}(E\lambda,\omega)|F(E\lambda,q,\omega)|\frac{\mathrm{d}B}{\mathrm{d}\omega}(E\lambda,\omega)$$

is possible. Here, ω is the excitation energy, Ω_e the solid angle of the spectrometer, σ_M the Mott cross section, λ the multipole order, P_f the fission probability, F the form factor and $\mathrm{d}B/\mathrm{d}\omega$ the strength function.

* Work supported by the State of Hesse within the Cluster Project ELEMENTS (Project ID 500/10.006) and by DFG (GRK 2128 AccelencE).
† dschneider@ikp.tu-darmstadt.de

ISBN: 978-3-95450-247-9 ISSN: 2673-5490 doi: 10.18429/JACoW-IPAC2024-WEPG83

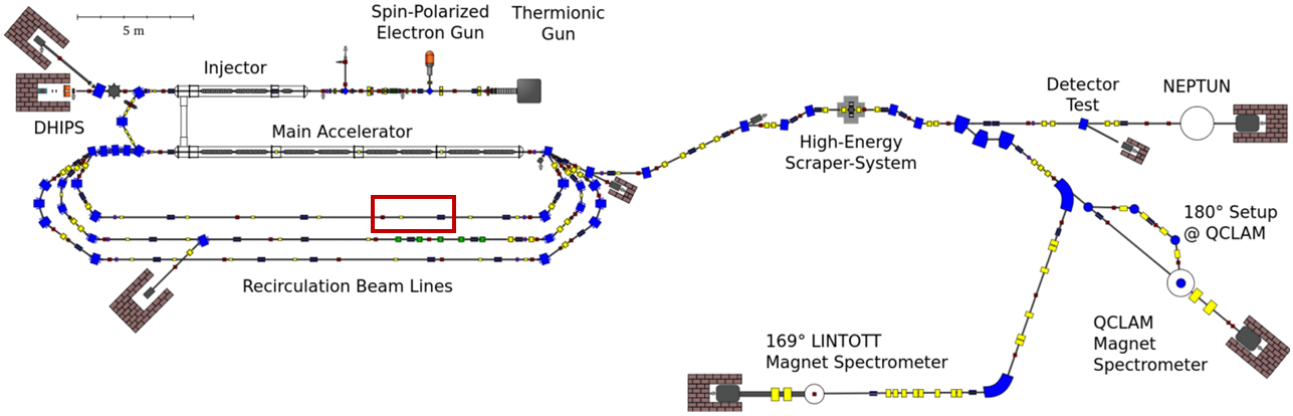

Figure 1: Floorplan of the S-DALINAC. Both the electrofission experiment and beam stabilization system will be located at the QCLAM magnet spectrometer. The commissioning measurement of the beam stabilization system has been conducted in the first recirculation beamline (location marked in red) [11].

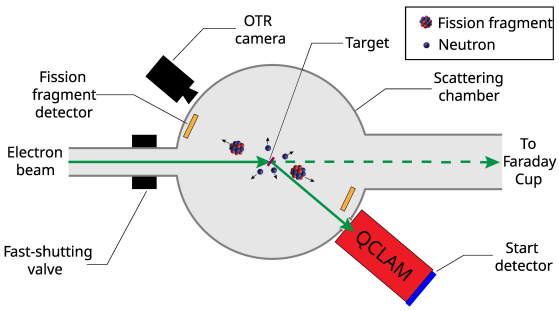

Figure 2: Schematic overview of the electrofission setup design. After interacting with an electron the target nucleus decays via fission. The fission fragments are detected in coincidence using double sided silicon strip detectors [13].

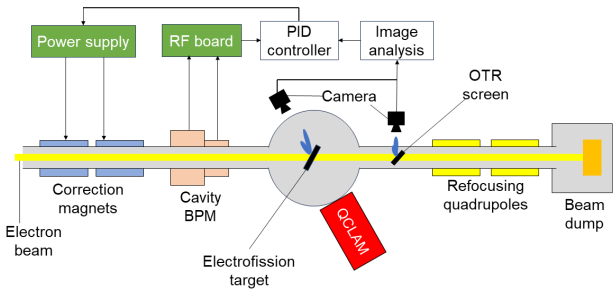

Figure 3: Design of the beam stabilisation system. OTR emitted by the electron beam at both the electrofission target and OTR screen is evaluated to determine the beam profile. A non-destructive measurement is deducted by a cavity BPM. The signal is processed by the control algorithm to adjust the correction magnet currents. Figure adapted from Ref. [13].

DESIGN OF THE BEAM STABILIZATION SYSTEM

The proposed electrofission experiment demands a high control and stability of beam parameters over a large measurement period. The design layout of the active beam-stabilization system matching those criteria is shown in Fig. 3. As the electron beam crosses the boundary between vacuum and actinide target material, optical transition radiation (OTR) is emitted [12]. The OTR is monitored with a camera providing the primary signal of the beam's transverse centroid for the control algorithm. Here, the resolution and frequency of the beam profile signal depends only on the OTR intensity, camera resolution and frame rate. The installed camera has a resolution of 22 µm per pixel. The upstream cavity beam position monitor (BPM) enables a non-destructive measurement of the beam's transverse centroid and bunch arrival phase giving access to the beam current and impact angle of the beam on the electrofission target. The downstream OTR screen serves for online beam diagnostics and initial beam tuning.

The signal of the cavity BPM is processed by a new generation of in-house developed radio frequency (RF) boards using amplitude detectors, In-phase and quadrature (I-Q) modulators and I-Q demodulators, providing signals at a rate of 100 Hz with a dynamic range of approx. 70 dB. The beam position resolution of the cavity BPM is expected to be better than 100 µm [14]. The OTR camera images are analyzed online utilizing 2D median filter and Gaussian fits, providing an exhaustive set of beam parameters based on both the raw pixel intensity distribution and the Gaussian fits. The accumulated beam parameters are fed into the Python-based control algorithm. The feedback control is based on a set of PI controllers with the control function

$$\Delta\xi(t) = K_{\mathrm{p},\xi}\,\xi(t) + K_{\mathrm{i},\xi}\int_0^t \xi(\tau)\,\mathrm{d}\tau \quad \text{with} \quad \xi \in \{x, y\}$$

aiming to stabilize the observed horizontal x and vertical beam position y for a given time t. Here, $\Delta\xi$ is the correction in position calculated by the PI controller and K_p and K_i denote the non-negative coefficients for the proportional and integral terms, respectively. The derivative term was chosen to be zero. As the beam stabilization system aims to mitigate beam distortions of < 1 Hz, most of the data transfer has been

ISBN: 978-3-95450-247-9 ISSN: 2673-5490 doi: 10.18429/JACoW-IPAC2024-WEPG83

realized via the Experimental Physics and Industrial Control System (EPICS) based control system [15]. This allows the application of the beam stabilization control algorithm to any given set of correction magnets and experimental target or diagnostic screen. In exchange, the feedback loop is limited to a frequency of up to approx. 10 Hz [16].

COMMISSIONING

The commissioning measurement of the beam stabilization system has been conducted in the first recirculation beamline during beam tuning. Due to the EPICS integration of the system, the existing correction magnets could be used to stabilize the beam's transverse centroid on a downstream Kapton-coated aluminum screen (see Fig. 1). The OTR emitted by the electrons passing the screen has been monitored with a camera at a 10 Hz frame rate. Here, the horizontal and vertical beam spot size during the commissioning has been determined to $\sigma_x = (475.2 \pm 8.4)$ µm and $\sigma_y = (414.3 \pm 7.5)$ µm, respectively, using Gaussian fits, and is therefore significantly larger than aimed for the electrofission experiment. Due to the processing time of both the image analysis algorithm and control algorithm, the feedback loop frequency was limited to 3 Hz. The cavity BPM shown in Fig. 3 was not available at the given location and is therefore not included.

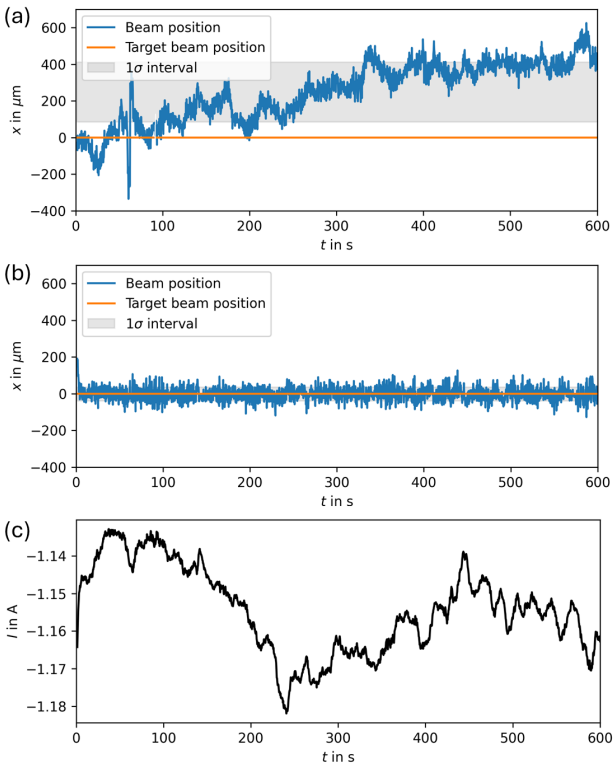

Figure 4: Beam's horizontal centroid x observed on a diagnostics screen with active beam-stabilization disabled (a) and enabled (b) in subsequent 10 minute runs. For the latter case the mitigation of beam drifts can be observed by plotting the correction magnet current I during the run (c).

First, a measurement without beam stabilization has been conducted. The observed beam's horizontal centroid shown in Fig. 4(a) serves as reference. Within a 600 s run, the beam's horizontal centroid has a mean displacement from the target position (set to 0) of $\bar{x}_{\text{off}} = (249.2 \pm 163.3)$ µm. The beam's horizontal centroid and correction magnet current with active control algorithm is shown in Fig. 4(b)-(c). Here, the parameters $K_{\text{p},x} = K_{\text{p},y} = 0.2$ and $K_{\text{i},x} = K_{\text{p},y} = 0.001$ of the PI controller have been found experimentally by minimizing the standard deviation of the beam position of subsequent runs. The beam's horizontal mean displacement has been reduced to $\bar{x}_{\text{on}} = (0.7 \pm 37.3)$ µm. In the vertical plane the beam's mean displacement has been improved from $\bar{y}_{\text{off}} = (151.5 \pm 114.7)$ µm to $\bar{y}_{\text{on}} = (0.4 \pm 28.7)$ µm. Therefore, shifts of the beam's position have been mitigated almost entirely. While the beam stabilization is active the monitored beam position does not provide information on whether beam distortions are present. The effect of the active beam-stabilization has been observed online by plotting the correction magnet current I indicating the mitigated beam distortions.

The control algorithm has been expanded by a function to calibrate and integrate the correction magnet current $I(\Delta\xi)$ as a function of the beam displacement $\Delta\xi$ to be compensated calculated by the PI controller. It is expected that the deduced PI parameters can therefore be applied to future beam stabilization applications at other locations at the S-DALINAC leading to less time-consuming PID fine-tuning measurements.

As surrogate models of accelerator subsystems have been proven effective in analyzing and refining the underlying system, it is currently in process to create such a system based on both simulations and machine-learning techniques like neural networks or polynomial chaos [17]. The constructed surrogate models will serve as training and testing environments for different control algorithms, such as PID controllers and supervised learning agents.

CONCLUSION

While the S-DALINAC is well suited to provide a high-quality electron beam for the upcoming electrofission experiment, the implementation of an active beam-stabilization system to ensure a stable on-target beam position for the given measurement period is required. In a first commissioning measurement the beam stabilization was able to mitigate drifts of the beam position almost entirely. Within the shown 600 s runs, the standard deviation of the beam's mean displacement has been reduced by a factor of approx. 5. Due to the large beam spot size during the commissioning in the first recirculation beamline a beam stabilization within a 1 mm diameter including the 3σ beam width has not yet been demonstrated. A demonstration measurement at the QCLAM magnet spectrometer utilizing the active beam-stabilization is therefore required. Additionally, a commissioning of the active beam-stabilization system including the cavity BPM is necessary.

ISBN: 978-3-95450-247-9 ISSN: 2673-5490 doi: 10.18429/JACoW-IPAC2024-WEPG83

REFERENCES

[1] N. Pietralla, "The Institute of Nuclear Physics at the TU Darmstadt", *Nucl. Phys. News*, vol. 28, no. 2, pp. 4–11, 2018. doi:10.1080/10619127.2018.1463013

[2] M. Arnold *et al.*, "First operation of the superconducting Darmstadt linear electron accelerator as an energy recovery linac", *Phys. Rev. Accel. Beams*, vol. 23, p. 020101, 2020. doi:10.1103/PhysRevAccelBeams.23.020101

[3] F. Schliessmann *et al.*, "Realization of a multi-turn energy recovery accelerator", *Nat. Phys.*, vol. 19, pp. 597–602, 2023. doi:10.1038/s41567-022-01856-w

[4] F. Schliessmann *et al.*, "Studies on a Triple-Turn Energy-Recovery Mode at the S-DALINAC", *J. Phys.: Conf. Ser.*, vol. 2687, p. 032023, 2024. doi:10.1088/1742-6596/2687/3/032023

[5] F. Hug, "Erhöhung der Energieschärfe des Elektronenstrahls am S-DALINAC durch nicht-isochrones Rezirkulieren", Ph.D. thesis, Technische Universität Darmstadt, Darmstadt, Germany, 2013. https://tuprints.ulb.tu-darmstadt.de/id/eprint/3469

[6] L. Jürgensen, "Entwicklung und Aufbau eines Hochenergie-Elektronen-Scrapersystems für den S-DALINAC", Ph.D. thesis, Technische Universität Darmstadt, Darmstadt, Germany, 2018. https://tuprints.ulb.tu-darmstadt.de/id/eprint/7489

[7] G. Steinhilber, "The electron-gamma coincidence set-up at the S-DALINAC" , Ph.D. thesis, Technische Universität Darmstadt, Darmstadt, Germany, 2023. doi:10.26083/tuprints-00022993

[8] C. Lüttge *et al.*, "Large-aperture system for high-resolution electron scattering", *Nucl. Instrum. Methods Phys. Res., Sect. A*, vol. 366, no. 2-3, pp. 325–331, 1995.

[9] U. Kneissl *et al.*, "Search for E2 strength in electrofission of 238U and 232Th", *Nucl. Phys. A*, vol. 256, no. 1, pp. 11–22, 1976. doi:10.1016/0375-9474(76)90091-9

[10] F. Zamani-Noor and D. S. Onley, "Virtual photon theory in electrofission", *Phys. Rev. C*, vol. 33, no. 4, pp. 1354–1366, 1986. doi:10.1103/PhysRevC.33.1354

[11] T. Bahlo, "Entwurf eines Mollerpolarimeters und Entwicklung einer aktiven Phasenstabilisierung für den Injektor des S-DALINAC", Ph.D. thesis, Technische Universität Darmstadt, Darmstadt, Germany, 2017. https://tuprints.ulb.tu-darmstadt.de/id/eprint/6849

[12] V. L. Ginzburg and I. M. Frank, "Radiation of a uniformly moving electron crossing a boundary between two media", *Phys. Rep.*, vol. 49 pp. 1-89, 1979.

[13] D. Schneider *et al.*, "Development of an Active Beam-Stabilization System for Electrofission Experiments at the S-DALINAC", in *Proc. IBIC'23*, pp. 111-114, 2023. doi:10.18429/JACoW-IBIC2023-MOP038

[14] S. Döbert, "Nichtlineare Zeitreihenanalyse der Feldamplitude der supraleitenden Beschleunigungsstrukturen und Aufbau eines HF-Monitorsystems zur zerstörungsfreien Strahldiagnose am S-DALINAC", Ph.D. thesis, Technische Universität Darmstadt, Darmstadt, Germany, 1999.

[15] EPICS – Experimental Physics and Industrial Control System. https://epics.anl.gov/

[16] M. Konrad, "Development and Commissioning of a Digital RF Control System for the S-DALINAC and Migration of the Accelerator Control System to an EPICS Based System", Ph.D. thesis, Technische Universität Darmstadt, Darmstadt, Germany, 2013. https://tuprints.ulb.tu-darmstadt.de/id/eprint/3398

[17] D. Schneider, "Sensitivitätsanalyse der Strahlführungselemente des S-DALINAC unter Anwendung von Polynom-Chaos", master thesis, Technische Universität Darmstadt, Darmstadt, Germany, 2021.